Chemical Science

ROYAL SOCIETY OF CHEMISTRY

EDGE ARTICLE

View Article Online
View Journal | View Issue

Cite this: *Chem. Sci.*, 2025, **16**, 9213

All publication charges for this article have been paid for by the Royal Society of Chemistry

Received 3rd February 2025
Accepted 15th April 2025

DOI: 10.1039/d5sc00872g

rsc.li/chemical-science

Photoinduced copper-catalysed enantioselective amination of allylic and propargylic C–H bonds†

Ling Dai, Ying-Ying Chen, Jing-Jun Wang, Jun-Jia Chen and Qi-Lin Zhou *

The hydrogen atom transfer (HAT)-mediated strategy has emerged as a straightforward and powerful approach for oxidative C–H bond functionalization. However, despite remarkable progress in this field, enantioselective allylic and propargylic C–H aminations remain a challenge. In this study, we developed highly enantioselective allylic and propargylic C–H aminations by combining a visible light-activated HAT process with copper catalysis. Using this method, a wide range of alkenes and alkynes can be converted into high-value chiral allylic and propargylic amines with high enantio-, regio-, and *E*/*Z*-selectivity. These enantio-enriched amines serve as versatile building blocks in organic synthesis and hold significant potential for applications in the synthesis of pharmaceuticals, natural products and other bioactive molecules.

Introduction

Chiral amines, particularly allylic amines, are ubiquitous structure motifs in pharmaceuticals, natural products, and other biologically active molecules (Scheme 1A).[1–3] Enantioselective C(sp^3)–H amination provides a straightforward approach for synthesizing chiral amines due to the abundant availability of starting materials and the elimination of substrate pre-activation.[4–6] Transition metal-catalysed C–H activation *via* π-allyl metal intermediates is an efficient method for the synthesis of chiral allylic amines;[7–10] however, successful examples of this method are limited to intramolecular reactions.[11,12] Metal-nitrenoid insertion into the C–H bond has been reported for achieving enantioselective allylic C–H amination,[13–18] but this catalytic system suffers from issues such as alkene isomerization, competing aziridination, and the requirement for pre-functionalized nitrene precursors (Scheme 1B).[19,20] Therefore, it is desirable to develop efficient and practical methods for enantioselective allylic C–H amination.[21]

Recently, the radical-mediated hydrogen-atom transfer (HAT) process has emerged as an efficient strategy for enantioselective C–H bond functionalization.[22–24] In 2022, Gevorgyan and co-workers presented an open-shell approach that enables palladium-catalysed enantioselective allylic C–H amination with nucleophilic aliphatic amines (Scheme 1C).[25] Nevertheless, the substrate scope remained relatively narrow, with only a few substrates achieving optimal enantioselectivity control. We have previously reported a copper-catalysed enantioselective benzylic C–H amination using peroxide as the HAT reagent and amides as amination reagents.[26] However, this cationic copper catalyst exhibited very low yield in the enantioselective allylic C–H amination of alkenes. Through a systematic investigation of various reaction parameters, we found that the reaction proceeds under visible light irradiation with carbamate as the amination reagent. Herein, we describe the photoinduced copper-catalysed enantioselective allylic C–H amination of alkenes, which produces chiral primary allylamines with high enantio-, regio-, chemo-, and *E*/*Z*-selectivity. Moreover, this strategy can also be successfully applied to enantioselective propargylic C–H amination (Scheme 1D).

Results & discussion

The copper-catalysed amination of (*E*)-but-1-ene-1-phenyl (**1a**) with methyl carbamate (**2a**) was carried out to find efficient catalysts, oxidants, amine sources, and optimal reaction conditions (Table 1, see Tables S1–S6† for details). A comparison of ligands showed that the Evans bisoxazoline ligand **L9** with bulky phenyl groups was the optimal ligand, producing amination product **3a** with high yield and enantioselectivity. The study of catalyst precursors revealed that the combination of CuCl and $NaBAr_F$ provided the best yield and enantioselectivity (entries 1–4, see Table S2† for details). Among the tested oxidants, di-*tert*-butyl peroxide (DTBP) offered the most satisfactory results, generating *tert*-butoxy radicals under visible light irradiation and subsequently alkyl radicals from alkenes *via* the HAT process[27,28] (entries 5, 6 *vs.* 1, see Table S3† for details). In addition to C_6F_6, in which the reaction has the highest yield and enantioselectivity, C_6H_5Cl and dichloroethane (DCE) were also viable solvents, albeit with lower yield and

State Key Laboratory and Institute of Elemento-Organic Chemistry, College of Chemistry, Frontiers Science Center for New Organic Matter, Nankai University, Tianjin 300071, China. E-mail: qlzhou@nankai.edu.cn

† Electronic supplementary information (ESI) available. CCDC 2378637. For ESI and crystallographic data in CIF or other electronic format see DOI: https://doi.org/10.1039/d5sc00872g

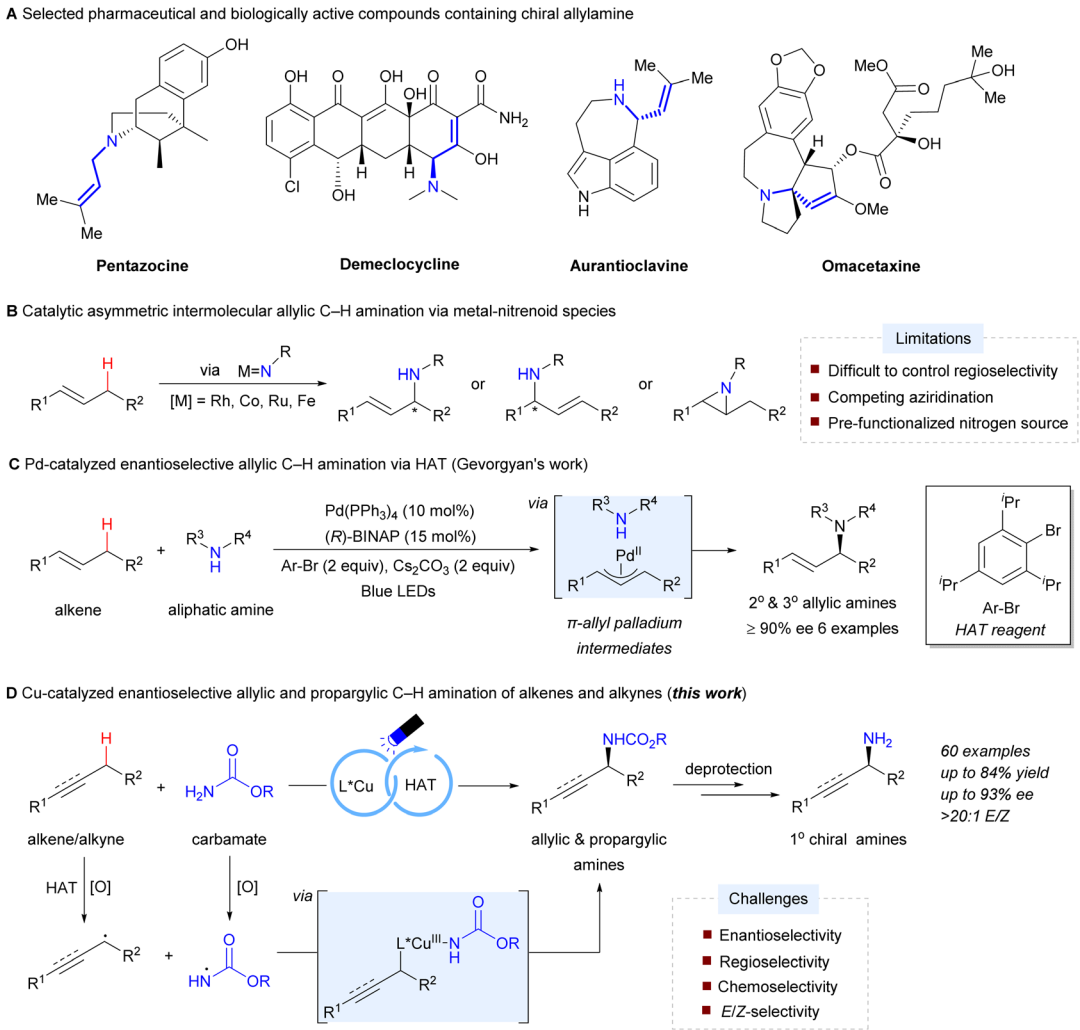

Scheme 1 Catalytic asymmetric allylic C–H amination reactions.

enantioselectivity (entries 7, 8 *vs.* 1). Control experiments demonstrated that each of the following components—copper, sodium tetrakis[3,5-bis(trifluoromethyl)phenyl] borate ($NaBAr_F$), ligand **L9**, DTBP, and light—is indispensable for the reaction (entries 9–13). The reaction was also successfully carried out with one equivalent of alkene, although the yield and enantioselectivity were slightly lower (entry 14).

Under optimal reaction conditions, we explored the substrate scope of alkenes and carbamates (Scheme 2). Alkene substrates **1**, whether as pure *E*-isomers or *E*/*Z* mixtures, reacted with carbamate **2a** to yield thermodynamically stable *E*-products **3** (*E*/*Z* > 20 : 1). The excellent *E*/*Z*-selectivity enhances the practicability of the reaction, as many alkenes are usually prepared as *E*/*Z*-mixtures. Alkenes with *para*-substituents on the benzene ring, regardless of whether they are electron-donating or electron-withdrawing, showed moderate to good yield and high enantioselectivity (≥90% ee) (**1a–1c**, **1e–1h**, and **1j–1l**). Exceptions included **1d** (with a *para*-F) and **1i** (with a *para*-MsO), which exhibited lower enantioselectivity (80% ee). Alkenes with *meta*-substituents on the benzene ring (**1m–1p**) afforded the desired amination products with 85–90% ee. However, those with *ortho*-halogen substituents (**1q** and **1r**) displayed lower enantioselectivity (82% ee and 80% ee, respectively). Similarly, substrates with 2-naphthyl (**1s**, 80% ee), benzofuran-5-yl (**1t**, 80% ee) and benzothiophen-5-yl (**1u**, 85% ee) also showed lower enantioselectivity. Notably, the reaction demonstrated good functional group compatibility with chlorine (**1x**), acetoxy (**1y**) and ester (**1z**) substituents on the alkyl chains of alkene substrates. Other carbamates, such as $BocNH_2$ (**2aa**), $CbzNH_2$ (**2ab**), $TeocNH_2$ (**2ac**) and $FmocNH_2$ (**2ad**), whose products are more easily deprotected, were also effective amine sources, affording good yields and high enantioselectivity (90–91% ee). The use of carbamates as amine sources provides convenience for the synthesis of allylic amines without a protecting group, as the alkyoxycarbonyl groups in the products can be removed by common methods.[29]

Encouraged by the success in the allylic C–H amination, we next studied the enantioselective propargylic C–H amination. We were delighted to find that the standard conditions for the allylic C–H amination also worked for the propargylic C–H amination reaction (Scheme 3). A variety of alkyl aryl alkynes with diverse substituents reacted with carbamate **2a** to yield the

Table 1 Optimization of reaction conditions

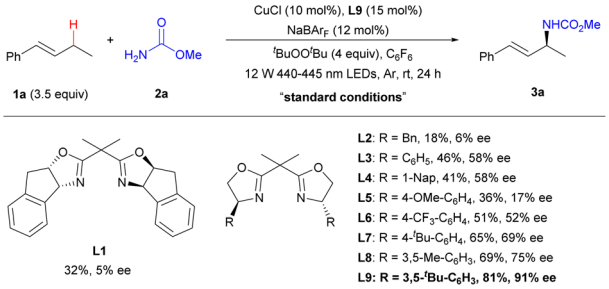

Entry	Variation from the "standard conditions"	Yield[a] (%)	ee[b] (%)
1	None	81 (76)[c]	91
2	$Cu(OTf)_2$ instead of CuCl/NaBAr$_F$	16	8
3	$Cu(CH_3CN)_4BF_4$ instead of CuCl/NaBAr$_F$	31	45
4	$Cu(CH_3CN)_4PF_6$ instead of CuCl/NaBAr$_F$	38	59
5	NFSI instead of DTBP	7	rac
6	DCP instead of DTBP	43	74
7	PhCl instead of C_6F_6	58	77
8	DCE instead of C_6F_6	62	86
9	Without CuCl	—	—
10	Without NaBAr$_F$	—	—
11	Without **L9**	—	—
12	Without DTBP	—	—
13	Without *hv*	—	—
14	1 equiv. of **1a**	52	87

[a] Yields were determined by ^{1}H NMR with dimethyl terephthalate as an internal standard. [b] Enantiomeric excess (ee) values were determined by chiral HPLC. [c] Isolated yield. NaBAr$_F$, sodium tetrakis [3,5-bis(trifluoromethyl)phenyl] borate. DTBP, di-*tert*-butyl peroxide. NFSI, *N*-fluorobenzenesulfonimide. DCP, dicumyl peroxide.

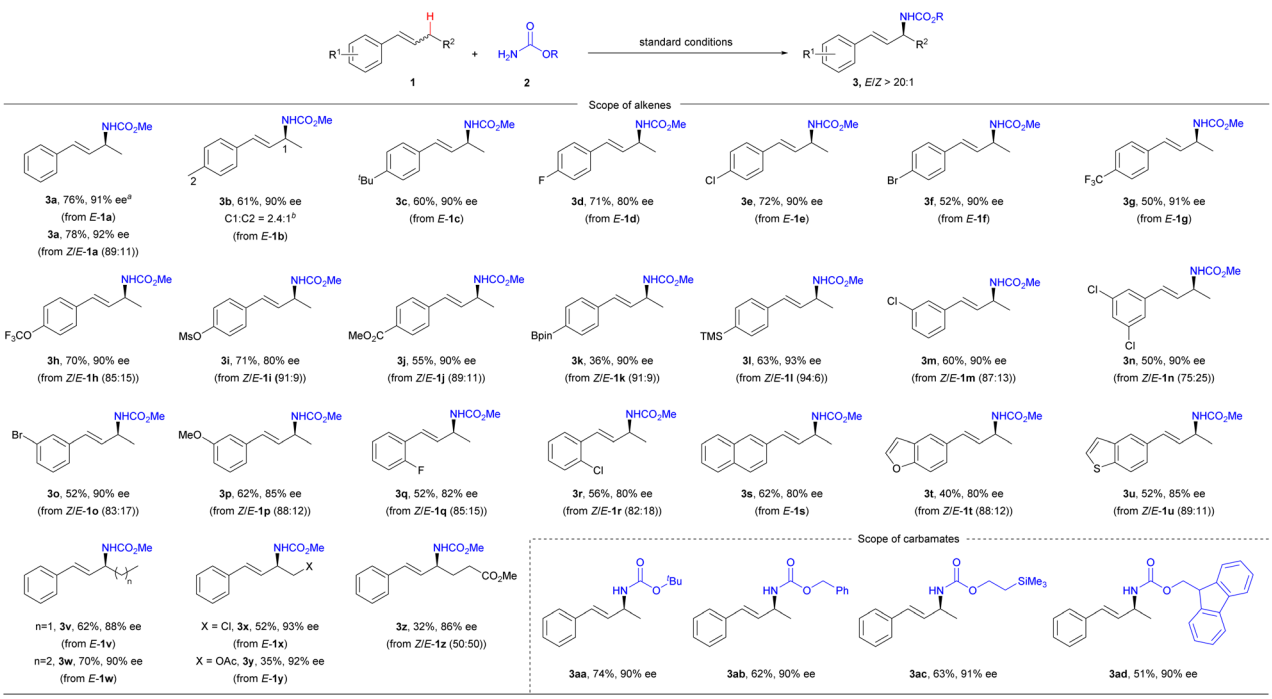

Scheme 2 Substrate scope of alkenes and carbamates. Isolated yield. Ee values were determined by chiral HPLC, and *E*/*Z* ratios were determined by ^{1}H NMR. [a]The absolute configuration of compound **3a** was determined to be *S* by comparing the optical rotation of its deprotected amine with that reported in the literature. [b]The ratio of site-isomers was determined by ^{1}H NMR. BocNH_2, *tert*-butyl carbamate. CbzNH_2, benzyl carbamate. TeocNH_2, 2-(trimethylsilyl)ethyl carbamate. FmocNH_2, (9*H*-fluoren-9-yl)methyl carbamate.

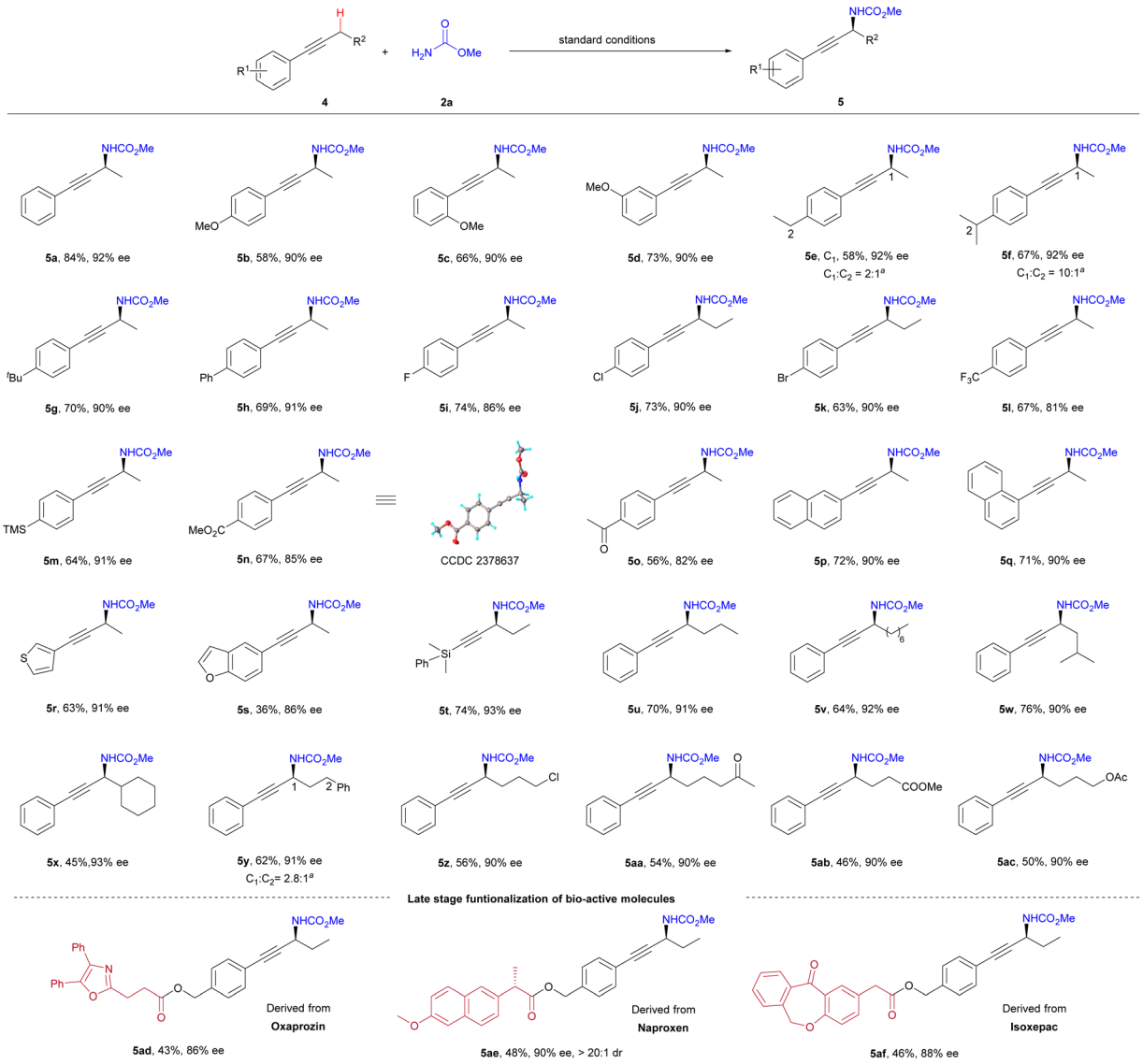

Scheme 3 Substrate scope of alkynes. Isolated yield, ee values were determined by chiral HPLC. [a]The ratio of site-isomers was determined by ^{1}H NMR.

propargylic C–H amination products (**5b–5o**) in good yields (56–84%) and with high enantioselectivities (81–92% ee). The amination selectively occurred at the propargylic site when the substrate contained both propargylic and benzylic C–H bonds (**5e** and **5f**). Alkyne substrates featuring naphthyl (**5p** and **5q**, 90% ee), 3-thienyl (**5r**, 91% ee), benzofuryl (**5s**, 86% ee), and silyl (**5t**, 93% ee) also demonstrated high enantioselectivity in the reaction. The effect of substrate's alkyl chain and its functional groups on the enantioselectivity was negligible, indicating the reaction's broad tolerance for functional groups (**5u–5ac**). Additionally, alkynes derived from oxaprozin (**4ad**), naproxen (**4ae**), and isoxepac (**4af**) reacted smoothly with **2a** to yield the corresponding propargylic amines with good enantioselectivity. The absolute configuration of **5n** was determined to be *S* by X-ray single crystal diffraction analysis.

To demonstrate the synthetic utility of the method, we investigated the transformations of the amination products (Scheme 4). The deprotection of amination products **3a** and **5ag** yielded chiral primary amines **6** [30] and **9**, without any loss of enantiopurity. Product **3a** was successfully converted into saturated aliphatic amine **7** and epoxide **8** by treatment with Pd–C/H_2 and *m*-CPBA, respectively. Similarly, the hydrogenation of product **5a** provided *Z*-allylamine **10**. Removal of the silyl group from product **5t** afforded terminal alkyne **11**, which is a versatile intermediate suitable for Sonogashira coupling or Click reactions. Lysophosphatidic acid receptor **13**, a compound used in the treatment of fibrotic diseases,[31] and anticancer agent **16** [32] were readily prepared using asymmetric amination as the key step, further showcasing the method's potential for pharmaceutical synthesis.

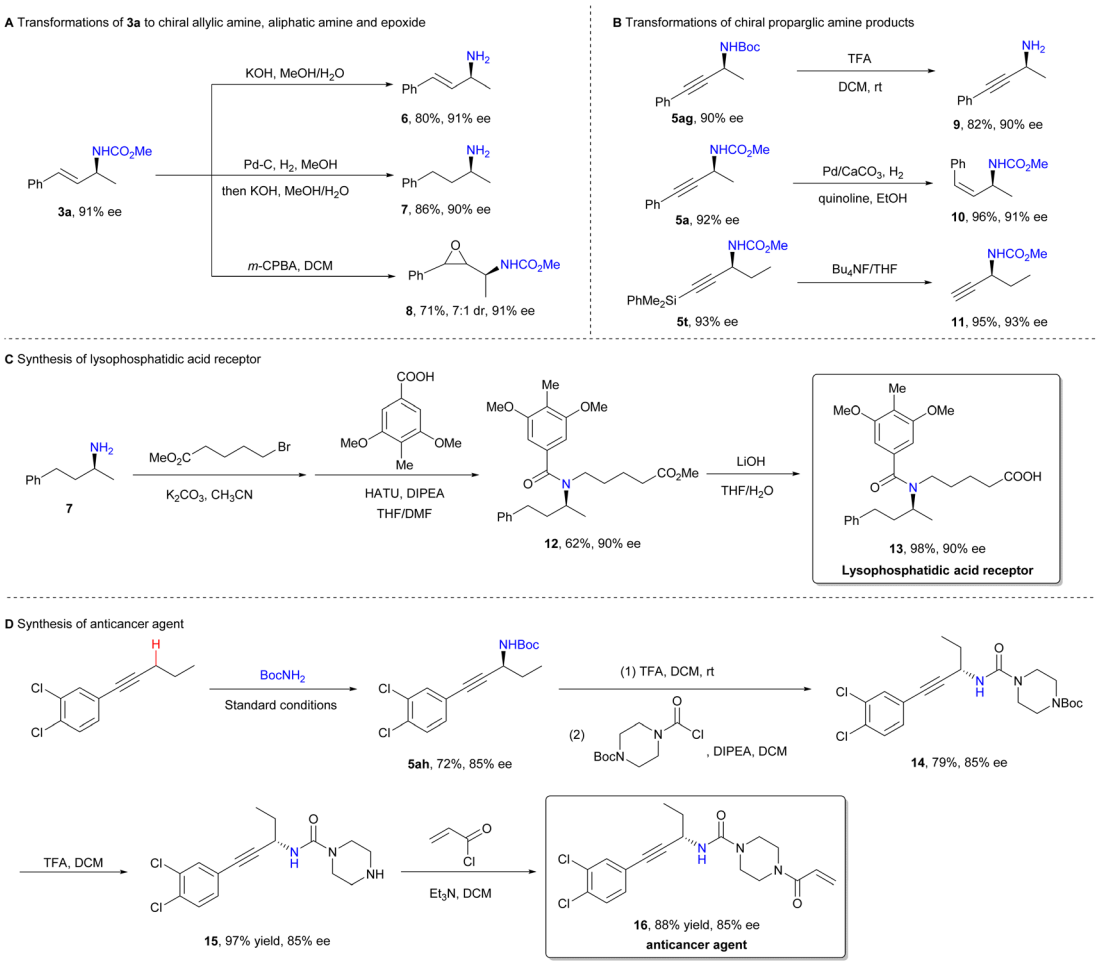

Scheme 4 Synthetic applications.

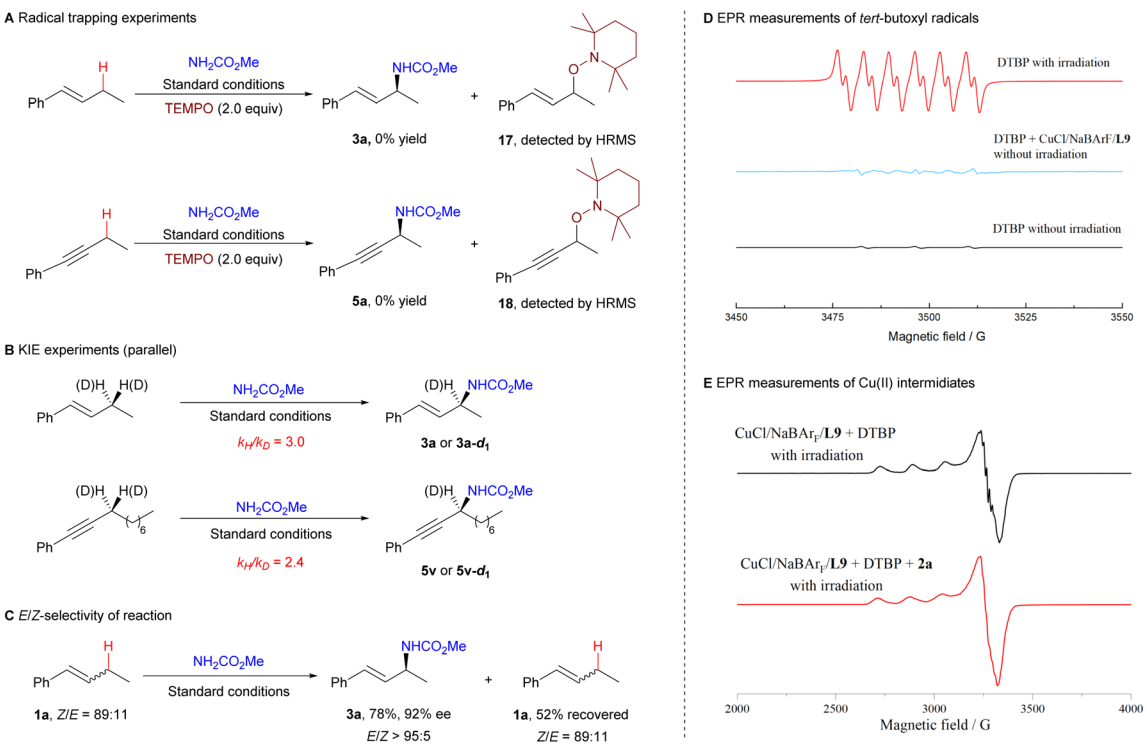

Scheme 5 Mechanism studies.

To gain insight into the reaction mechanism, we conducted several experiments to identify the key intermediates of the reaction (Scheme 5). Under the standard conditions, the addition of the radical scavenger 2,2,6,6-tetramethyl-1-piperidinyloxy (TEMPO) completely inhibited the reaction (Scheme 5A), indicating the involvement of a free radical process. Deuterium kinetic isotope effect (KIE) experiments yielded KIE values of 3.0 and 2.4, suggesting that the hydrogen atom abstraction from the C(sp^3)–H bond by a *tert*-butoxy radical might likely be the rate-limiting step (Scheme 5B). When substrate **1a** and product **3a** were exposed to visible light irradiation, no carbon–carbon double bond isomerization was observed (see the ESI† for details), and the *E*/*Z* ratio of the alkene substrate **1a** remained unchanged during the reaction (Scheme 5C). These results supported that the *E*-selection in the allylic C–H amination reaction might be generated through a stereospecific amination of the allyl-copper intermediate, rather than through a photoinduced double bond isomerization process. Using electron paramagnetic resonance (EPR) with the spin-trapping agent 5,5-dimethyl-1-pyrrolidine *N*-oxide (DMPO), we detected *tert*-butoxy radicals and found that these radicals are primarily generated by visible light irradiation (Scheme 5D).[33] A copper(II) signal was observed in the EPR measurements of the reaction mixture, indicating that copper(II) species, such as Cu^{II}–O^{t}Bu or Cu^{II}–$NHCO_2Me$ intermediates, may be involved in the reaction[34,35] (Scheme 5E).

Based on our experimental results and previous reports,[22–24] we propose a mechanism for the enantioselective allylic C–H amination, as shown in Scheme 6. Upon visible light irradiation, DTBP decomposes to generate *tert*-butoxy radicals, which react with the cationic copper(I) complex **A** to form the Cu(II)–O^{t}Bu intermediate **B**. Ligand exchange of **B** with carbamate **2a** yields the Cu(II)–$NHCO_2Me$ intermediate **C**. Intermediate **C** interacts with the allyl radical, which is generated by the abstraction of the allylic hydrogen from **1a** by the *tert*-butoxy radical, to form the copper(III) intermediate **D**. Subsequently, **D** undergoes reductive elimination, producing product **3a** and regenerating the copper(I) complex **A**.

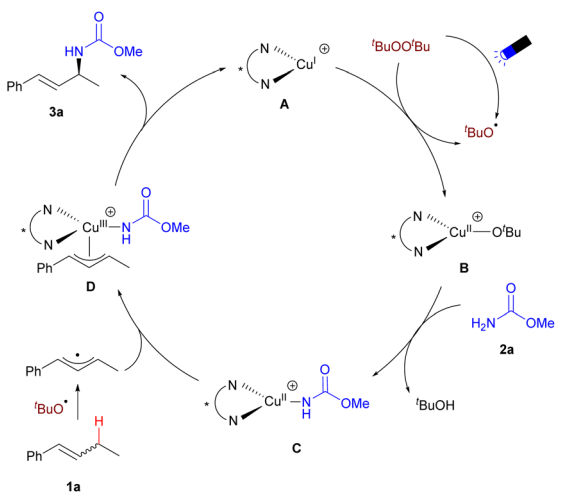

Scheme 6 Plausible mechanism of allylic C–H amination.

Conclusions

In summary, we have developed a photoinduced copper-catalysed enantioselective C–H amination of alkenes and alkynes. This reaction enables the efficient synthesis of diverse chiral allylic amines and propargylic amines with high enantioselectivity, regioselectivity, and *E*/*Z*-selectivity. Mechanistic studies of the reaction reveal that visible-light irradiation decomposes DTBP to generate *tert*-butoxy radicals, which play a key role in the HAT process and in maintaining the Cu(I)–Cu(II)–Cu(III) catalytic cycle. The protocol shows great potential for applications in the synthesis of bioactive compounds. Future efforts will focus on applying this strategy to other enantioselective C(sp^3)–H functionalizations.

Data availability

The data supporting this article have been included in the ESI.† Crystallographic data for compound **5n** have been deposited at the Cambridge Crystallographic Data Centre, reference numbers CCDC: 2378637.

Author contributions

Q.-L. Z. conceived the study; L. D. and Q.-L. Z. designed the experiments and analyzed the data; L. D., Y.-Y. C., J.-J. W. and J.-J. C. prepared substrates and ligands. L. D. performed the reactions and mechanistic study. L. D. and Q.-L. Z. wrote the manuscript.

Conflicts of interest

There are no conflicts to declare.

Acknowledgements

We thank the National Key R&D Program of China (2022YFA1504302), the National Natural Science Foundation of China (22188101 and 91956000), the Fundamental Research Funds for the Central Universities, and the Haihe Laboratory of Sustainable Chemical Transformations for financial support.

Notes and references

1 A. Stütz, *Angew. Chem., Int. Ed.*, 1987, **26**, 320–328.
2 G. Petranyi, N. S. Ryder and A. Stütz, *Science*, 1984, **224**, 1239–1241.
3 M. Johannsen and K. A. Jorgensen, *Chem. Rev.*, 1998, **98**, 1689–1708.
4 Y. Park, Y. Kim and S. Chang, *Chem. Rev.*, 2017, **117**, 9247–9301.
5 T. A. Ramirez, B. Zhao and Y. Shi, *Chem. Soc. Rev.*, 2012, **41**, 931–942.
6 F. Collet, C. Lescot and P. Dauban, *Chem. Soc. Rev.*, 2011, **40**, 1926–1936.
7 S. A. Reed and M. C. White, *J. Am. Chem. Soc.*, 2008, **130**, 3316–3318.

8 G. Liu, G. Yin and L. Wu, *Angew. Chem., Int. Ed.*, 2008, **47**, 4733–4736.
9 H. Lei and T. Rovis, *Nat. Chem.*, 2020, **12**, 725–731.
10 Y. Jin, Y. Jing, C. Li, M. Li, W. Wu, Z. Ke and H. Jiang, *Nat. Chem.*, 2022, **14**, 1118–1125.
11 P.-S. Wang, M.-L. Shen, T.-C. Wang, H.-C. Lin and L.-Z. Gong, *Angew. Chem., Int. Ed.*, 2017, **56**, 16032–16036.
12 Y. Bunno, Y. Tsukimawashi, M. Kojima, T. Yoshino and S. Matsunaga, *ACS Catal.*, 2021, **11**, 2663–2668.
13 Y. Nishioka, T. Uchida and T. Katsuki, *Angew. Chem., Int. Ed.*, 2013, **52**, 1739–1742.
14 P. Xu, J. Xie, D.-S. Wang and X. P. Zhang, *Nat. Chem.*, 2023, **15**, 498–507.
15 L.-M. Jin, P. Xu, J. Xie and X. P. Zhang, *J. Am. Chem. Soc.*, 2020, **142**, 20828–20836.
16 C. M. B. Farr, A. M. Kazerouni, B. Park, C. D. Poff, J. Won, K. R. Sharp, M.-H. Baik and S. B. Blakey, *J. Am. Chem. Soc.*, 2020, **142**, 13996–14004.
17 C. Liang, F. Collet, F. Robert-Peillard, P. Müller, R. H. Dodd and P. Dauban, *J. Am. Chem. Soc.*, 2008, **130**, 343–350.
18 H. Ahmed, B. Ghosh, S. Breitenlechner, M. Feßner, C. Merten and T. Bach, *Angew. Chem., Int. Ed.*, 2024, **63**, e202407003.
19 J. L. Roizen, M. E. Harvey and J. Du Bois, *Acc. Chem. Res.*, 2012, **45**, 911–922.
20 H. Lei and T. Rovis, *J. Am. Chem. Soc.*, 2019, **141**, 2268–2273.
21 Z.-J. Jia, S. Gao and F. H. Arnold, *J. Am. Chem. Soc.*, 2020, **142**, 10279–10283.
22 Z. Zhang, P. Chen and G. Liu, *Chem. Soc. Rev.*, 2022, **51**, 1640–1658.
23 D. L. Golden, S.-E. Suh and S. S. Stahl, *Nat. Rev. Chem.*, 2022, **6**, 405–427.
24 C. Zhang, Z.-L. Li, Q.-S. Gu and X.-Y. Liu, *Nat. Commun.*, 2021, **12**, 475–483.
25 K. P. S. Cheung, J. Fang, K. Mukherjee, A. Mihranyan and V. Gevorgyan, *Science*, 2022, **378**, 1207–1213.
26 L. Dai, Y.-Y. Chen, L.-J. Xiao and Q.-L. Zhou, *Angew. Chem., Int. Ed.*, 2023, **62**, e202304427.
27 Y.-W. Zheng, R. Narobe, K. Donabauer, S. Yakubov and B. König, *ACS Catal.*, 2020, **10**, 8582–8589.
28 D. L. Golden, C. Zhang, S.-J. Chen, A. Vasilopoulos, I. A. Guzei and S. S. Stahl, *J. Am. Chem. Soc.*, 2023, **145**, 9434–9440.
29 Y.-F. Zhang, X.-Y. Dong, J.-T. Cheng, N.-Y. Yang, L.-L. Wang, F.-L. Wang, C. Luan, J. Liu, Z.-L. Li, Q.-S. Gu and X.-Y. Liu, *J. Am. Chem. Soc.*, 2021, **143**, 15413–15419.
30 T. Tsunoda, O. Sasaki, O. Takeuchi and S. Itô, *Tetrahedron*, 1991, **47**, 3925–3934.
31 L. A. Black, W. H. Bunnelle, D. Chen, B. Clapham, D. A. Degoey, X. Deng, L. Fu, L. A. Hazelwood, L. Kong, Q. Lang, C.-H. Lee, M. Li, G. L. Lundgaard, M. V. Patel, R. Tao, L. Zhang, Q. Zang, Q. Zheng and W. Zhu, *US Pat.*, 2017177004A1, 2017.
32 D. Chikkanna, V. V. Khairnar, M. Ramachandra and K. Satyam, *IN Pat.*, 2019142126A1, 2010.
33 J. Hartung, K. Daniel, T. Gottwald, A. Gros and N. Schneiders, *Org. Biomol. Chem.*, 2006, **4**, 2313–2322.
34 M. M. Melzer, S. Mossin, X. Dai, A. M. Bartell, P. Kapoor, K. Meyer and T. H. Warren, *Angew. Chem., Int. Ed.*, 2010, **49**, 904–907.
35 S. Wiese, Y. M. Badiei, R. T. Gephart, S. Mossin, M. S. Varonka, M. M. Melzer, K. Meyer, T. R. Cundari and T. H. Warren, *Angew. Chem., Int. Ed.*, 2010, **49**, 8850–8855.